

# Radiative lifetimes and transition probabilities of astrophysical interest in Zr II

G. Malcheva,<sup>1</sup> K. Blagoev,<sup>1</sup> R. Mayo,<sup>2</sup> M. Ortiz,<sup>2</sup> H. L. Xu,<sup>3</sup> S. Svanberg,<sup>3</sup> P. Quinet<sup>4,5</sup> and E. Biémont<sup>4,5</sup>\*

<sup>1</sup>*Institute of Solid State Physics, 72 Tzarigradsko Chaussee, BG-1784 Sofia, Bulgaria*

<sup>2</sup>*Department of Atomic, Molecular and Nuclear Physics, Univ. Complutense de Madrid, E-28040 Madrid, Spain*

<sup>3</sup>*Department of Physics, Lund Institute of Technology, PO Box 118, S-221 00 Lund, Sweden*

<sup>4</sup>*IPNAS (Bât. B15), University of Liège, Sart Tilman, B-4000 Liège, Belgium*

<sup>5</sup>*Astrophysics and Spectroscopy, University of Mons-Hainaut, B-7000 Mons, Belgium*

Accepted 2005 December 14. Received 2005 December 12; in original form 2005 December 19

## ABSTRACT

Radiative lifetimes of 16 odd levels belonging to the  $4d^25p$  configuration of Zr II have been measured using a time-resolved laser-induced fluorescence technique with a single-step excitation process either from the ground state or from metastable levels belonging to the  $4d^25s$  and  $4d^3$  configurations. For 12 levels, there were no previous results available. The new experimental results and the lifetime values available in the literature have allowed to test a theoretical relativistic Hartree–Fock (HFR) model including core-polarization effects and to deduce transition probabilities for 242 transitions of astrophysical interest in the range 187.8–535.0 nm.

**Key words:** atomic data – atomic processes – methods: laboratory.

## 1 INTRODUCTION

The determination of elemental abundances in the stars, including the sun, requires a large number of accurate radiative transition probabilities. In the particular case of the chemically peculiar stars of the upper main sequence, large overabundances of many elements (including Zr) are deduced from the observed intensities of spectral lines and are generally explained in terms of diffusion processes in the outer layers of the stars. A precise determination of the enhancement factor of these abundances requires accurate oscillator strengths which are the key parameters in quantitative stellar abundances analyses. In addition, the yttrium anomaly (deviation from the odd–even effect, Y being more abundant than Sr and Zr in some chemically peculiar stars) and the importance of the Sr–Y–Zr patterns among these stars has often been pointed out in the literature (see e.g. Cowley & Aikman 1975 or Cowley 1976). As a consequence, a detailed knowledge of the Zr II spectrum (more generally of the zirconium spectrum and line intensities in the first three ionization stages) is of utmost importance in this context.

In astrophysics, Zr II has been observed in different types of stars including, e.g. the Ap stars of the Cr–Eu–Sr subgroup (Adelman 1973; Sadakane 1976) or the Bp stars of the Hg–Mn subgroup (Kodaira & Takada 1978). Zr II is also present and has been investigated in detail in the solar photosphere (see e.g. Biémont et al. 1981; Bogdanovich et al. 1995). Recent observations with the *Hubble Space Telescope* have raised the need for accurate radiative pa-

rameters for heavy atoms in different ionization stages. As an example, the Zr II and Zr III spectral lines in the ultraviolet (UV) spectral region have been observed in emission in the Hg–Mn star  $\chi$ -Lupi. Using a limited set of accurate oscillator strengths (26 transitions), Sikström et al. (1999) were unable to resolve the anomaly existing in this star between the local thermodynamic equilibrium (LTE) values of the zirconium abundance as deduced from weak lines of Zr II at optical wavelengths and strong Zr III lines appearing in the UV region. According to these authors, the difference is too large to be explained by uncertainties in the oscillator strengths and should be found probably in the stellar models (non-LTE effects or diffusion effects). However, an extended set of accurate atomic data in these ions is clearly most welcome for definitively assessing the origin of this zirconium conflict.

For these different reasons, the determination of transition probabilities in Zr II is timely in order to meet the needs of the astrophysicists interested in the determination of abundances in the stars.

## 2 PREVIOUS WORK

Zirconium has five stable isotopes, four of them (90, 91, 92 and 94) being produced in nucleosynthesis by the s process, the other one (96) being made by the r process. Zr is a very refractory element, difficult to vaporize by conventional thermal means and, consequently, has been relatively little investigated in the past.

The experimental transition probabilities reported by Corliss & Bozman (1962) for Zr II have been widely used in the astronomical literature but, since their publication, they have been shown to contain significant excitation-, wavelength- and intensity-dependent errors (see e.g. Bell & Upson 1971; Corliss & Tech 1976). More

\*E-mail: E. Biemont@ulg.ac.be

recently, the beam–foil method was used for measuring radiative lifetimes of two low-lying levels within the  $z^4 G^\circ$  multiplet (Poulsen et al. 1982). However, the lack of oscillator strengths for Zr II has motivated the deduction of radiative parameters from the analysis of stellar or solar spectra (see e.g. Boyarchuk & Boyarchuk 1960; Allen 1976; Luck & Bond 1981; Thevenin 1989, 1990; Meylan et al. 1993). For similar reasons, simple empirical formulae for the calculation of gf values were also proposed by Cowley (1983) and Cowley & Corliss (1983).

Some theoretical attempts to deduce transition probabilities and to fill in the gaps existing in the field have been reported by Malloy & Czyzak (1978), Pirronello & Strazzulla (1980) or Bogdanovich et al. (1995) but these publications contain data for only a limited number of transitions. In the latter case for example, 15 transitions only have been considered in Zr II and, in addition, these authors report large discrepancies observed between the length and velocity forms of the transition probabilities (reaching a factor of 2 in the case of the  $4d^3-4d^25p$  transitions) indicating that the model adopted could probably be improved.

‘Modern’ transition probability determination in Zr II, based on laser lifetime measurements combined with branching fractions (BFs) determination, includes the works of Hannaford & Lowe (1981), Biémont et al. (1981), Langhans, Schade & Helbig (1995) and Sikström et al. (1999). In the first cases (Biémont et al. 1981; Hannaford & Lowe 1981), a lifetime method based on fluorescence decay measurement following pulsed laser excitation of sputtered metal vapour was used in combination with measurements of BFs. As a direct consequence, accurate transition probabilities have been derived for 52 Zr II lines observed in the spectra of CP stars of the upper main sequence (Grevesse et al. 1981). These new data have been used to normalize the Sr–Y–Zr abundances in a large number of stars. The work of Langhans et al. (1995) was restricted to lifetime measurements with picosecond laser-induced fluorescence (LIF) spectroscopy combined with a pulsed hollow cathode discharge. In the paper of Sikström et al. (1999), six lifetimes were measured with time-resolved LIF spectroscopy. BFs were determined experimentally for 26 UV transitions depopulating three high-lying odd levels (situated at 55 834, 57 062 and 57 740  $\text{cm}^{-1}$ ).

An extension of previous sets of transition probabilities available in Zr II is thus needed and justified. In the present contribution, we report on transition probabilities for 243 transitions in the spectral range between 187.8 and 535.0 nm.

### 3 LIFETIME MEASUREMENTS

The ground term of Zr II is  $[\text{Kr}]4d^2(a^3F)5s^4F$ . Radiative lifetimes of 16 levels belonging to the  $4d^25p$  configurations (odd parity) were measured using a time-resolved LIF technique with a single-step excitation process either from the ground state or from appropriate metastable states belonging to the  $4d^25s$  and  $4d^3$  configurations. The experimental set-up used for the lifetime measurements has been discussed in detail elsewhere (see e.g. Biémont et al. 2004; Xu et al. 2004). Only a brief description is given here.

Free singly ionized zirconium atoms were obtained in a laser-produced plasma using a sample with natural isotopes. The Zr plasma contains neutral atoms, as well as ions in different ionization stages and has a layer structure in which the higher ionization stages are produced in the outer part of the cloud. The singly ionized atoms could be selected for the excitation by adjusting the delay time between the plasma production and excitation pulses. The excitation pulse had a duration of about 1 ns, and was obtained by compression in water with a stimulated Brillouin scattering device.

**Table 1.** Levels measured in Zr II and the corresponding excitation schemes.

State <sup>a</sup>	$E$ ( $\text{cm}^{-1}$ ) <sup>a</sup>	Origin ( $E$ in $\text{cm}^{-1}$ ) <sup>a</sup>	Excitation $\lambda$ (nm) <sub>vac.</sub>	Scheme	Detection $\lambda$ (nm) <sub>vac.</sub>
$z^2F^\circ_{5/2}$	29 504.97	2895.05	375.80	$2\omega + S$	342
$z^2F^\circ_{7/2}$	30 561.75	314.67	330.61	$2\omega$	373
$y^2F^\circ_{7/2}$	37 787.59	2895.05	286.59	$2\omega + A$	270
$x^2F^\circ_{7/2}$	42 504.11	314.67	237.03	$3\omega + S$	256
$x^2F^\circ_{5/2}$	42 860.72	0.0	233.31	$3\omega + S$	259
$y^2D^\circ_{3/2}$	32 983.73	2572.21	328.82	$2\omega$	366
$y^2D^\circ_{5/2}$	33 419.45	2572.21	324.18	$2\omega$	367
$x^2D^\circ_{3/2}$	41 467.72	0.0	241.15	$3\omega + S$	280
$x^2D^\circ_{5/2}$	41 676.82	0.0	239.94	$3\omega + S$	284
$z^2G^\circ_{9/2}$	35 185.64	3757.66	318.19	$2\omega$	348
$y^2G^\circ_{7/2}$	40 852.74	1322.91	252.97	$3\omega + 2S$	305
$z^2S^\circ_{1/2}$	34 810.03	2572.21	310.19	$2\omega$	344
$z^2P^\circ_{1/2}$	36 196.57	0.0	276.27	$2\omega + A$	313
$x^2P^\circ_{3/2}$	45 568.21	0.0	219.45	$3\omega$	264
$y^4P^\circ_{3/2}$	42 893.54	314.67	234.858	$3\omega + S$	287
$y^4P^\circ_{5/2}$	43 202.45	314.67	233.166	$3\omega + S$	284

<sup>a</sup>From Moore (1958).

$2\omega$  means the second harmonic, S and AS are written for the first Stokes and anti-Stokes components of stimulated Raman scattering.

The excitation process was performed in a vacuum chamber with a background pressure of  $10^{-6}$  to  $10^{-5}$  mbar. The ionic beam of zirconium is intersected at right angles by the pulsed laser beam tuned to a resonant transition of the upper state of interest. In order to obtain the required excitation wavelengths, different non-linear optical techniques, such as frequency upconversion in crystals, and stimulated Raman scattering technique in hydrogen gas, were applied. The excitation schemes for all the measured upper levels are described in Table 1.

The spectral lines were separated with a grating monochromator (resolution  $6.4 \text{ nm mm}^{-1}$ ) and the LIF signal was registered by a fast photomultiplier (Hamamatsu R1564U).

The measured lifetimes fall in the range from 2 to 9 ns. For the short-lived excited states, the temporal shape of the exciting laser pulses had to be considered. The decay curves were treated by a deconvolution process of the fluorescence signal and an excitation pulse recorded by inserting a metal rod into the excitation beam after the ablation pulse was blocked. A typical experimental curve for the  $y^4P^\circ_{5/2}$  state of Zr II is illustrated in Fig. 1 where the laser excitation pulse is also shown. The convolution fit gives a lifetime of  $2.6 \pm 0.2$  ns. The decay curves were registered by a fast digital recorder (Tektronix Model DSA 602) and result from the averaged fluorescence photons from 1000 pulses. Measurements under different physical conditions were performed to avoid systematic errors. A magnetic field of about 100 G, provided by a pair of Helmholtz coils, was also added and removed to detect eventual Zeeman quantum beats. Radiation trapping and collisional effects were checked by adjusting the plasma temperature and density, which could be achieved by varying the delay time and the ablation laser intensity. The delay times were chosen in the interval 1.5–4  $\mu\text{s}$  and no observable effects were found. About 10 curves were recorded for each level under study.

The experimental lifetime results of 16 excited states of Zr II and their corresponding uncertainties are summarized in Table 2 where they are compared with previous experimental results. For 12 of them there were no results previously available. The quoted error

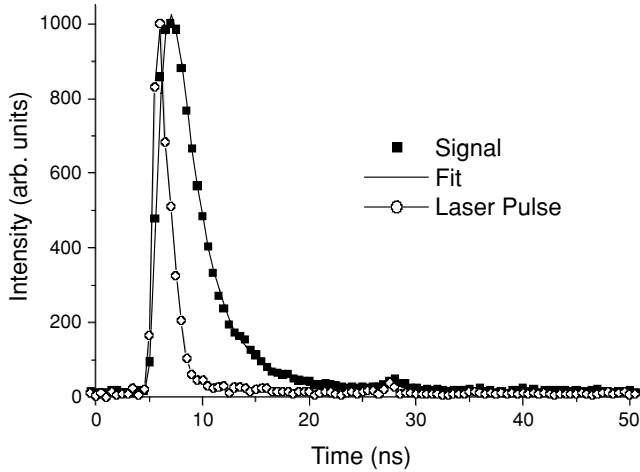


**Figure 1.** A typical experimental curve for the  $y\ 4P^{\circ}_{5/2}$  state of Zr II with a laser pulse. The convolution fit gives a lifetime of  $2.6 \pm 0.2$  ns.

**Table 2.** Experimental and theoretical radiative lifetimes ( $\lambda$ , in ns) in Zr II.

E (cm <sup>-1</sup> ) <sup>a</sup>	Designation <sup>a</sup>	$\tau$ (experiment)		$\lambda$ (theory)	
		Previous work	This work	Previous work	This work
27 983.83	$z\ 4G^{\circ}_{5/2}$	$7.1 \pm 0.2^b, 7.1 \pm 0.3^c$		6.1	
28 909.04	$z\ 4G^{\circ}_{7/2}$	$6.0 \pm 0.3^b$		5.5	
29 504.97	$z\ 2F^{\circ}_{5/2}$	$8.0 \pm 0.2^b$	$7.9 \pm 0.4$	7.0	
29 777.60	$z\ 4F^{\circ}_{3/2}$	$6.3 \pm 0.3^b$		5.0	
29 839.87	$z\ 4G^{\circ}_{9/2}$	$5.75 \pm 0.20^b, 7.6 \pm 1.0^d$		5.1	
30 435.38	$z\ 2D^{\circ}_{3/2}$	$7.2 \pm 0.3^b$		6.5	
30 551.48	$z\ 4F^{\circ}_{5/2}$			4.3	
30 561.75	$z\ 2F^{\circ}_{7/2}$	$8.2 \pm 0.4^b$	$7.9 \pm 0.4$	6.9	
30 795.74	$z\ 4G^{\circ}_{11/2}$	$5.4 \pm 0.4^e, 6.5 \pm 1.0^d$		4.8	
31 160.04	$z\ 2D^{\circ}_{5/2}$	$8.4 \pm 0.4^b$		7.4	
31 249.28	$z\ 4F^{\circ}_{7/2}$	$4.65 \pm 0.20^b, 4.7 \pm 0.3^e$		4.0	
31 866.49	$z\ 4F^{\circ}_{9/2}$	$4.55 \pm 0.20^b$		3.9	
31 981.25	$z\ 4D^{\circ}_{1/2}$	$7.1 \pm 0.3^f, 6.7 \pm 0.2^b$		5.5	
32 256.71	$z\ 4D^{\circ}_{3/2}$	$6.9 \pm 0.2^f, 6.9 \pm 0.4^e$		5.6	
32 614.71	$z\ 4D^{\circ}_{5/2}$	$7.0 \pm 0.3^f, 7.0 \pm 0.2^b$		5.7	
32 899.46	$z\ 4D^{\circ}_{7/2}$	$6.8 \pm 0.2^f$		5.3	
32 983.73	$y\ 2D^{\circ}_{3/2}$	$8.6 \pm 0.3^b$	$8.6 \pm 0.6$	7.8	
33 419.45	$y\ 2D^{\circ}_{5/2}$		$8.8 \pm 0.4$	7.6	
34 485.42	$z\ 2G^{\circ}_{7/2}$	$4.8 \pm 0.3^b$		4.1	
34 810.03	$z\ 2S^{\circ}_{1/2}$		$4.1 \pm 0.2$	3.6	
35 185.64	$z\ 2G^{\circ}_{9/2}$		$4.7 \pm 0.4$	4.1	
35 914.81	$z\ 2P^{\circ}_{3/2}$	$3.9 \pm 0.3^b$		2.9	
36 196.57	$z\ 2P^{\circ}_{1/2}$		$3.7 \pm 0.2$	3.1	
36 237.04	$y\ 4D^{\circ}_{1/2}$	$3.4 \pm 0.2^f$		3.5	
36 451.79	$y\ 4F^{\circ}_{3/2}$	$4.7 \pm 0.2^f, 4.9 \pm 0.2^b$		5.5	
36 638.50	$y\ 4D^{\circ}_{3/2}$	$3.2 \pm 0.2^f, 3.9 \pm 0.2^b$		3.5	
36 869.00	$y\ 4F^{\circ}_{5/2}$	$4.4 \pm 0.2^f, 4.6 \pm 0.2^b$		5.0	
37 171.22	$y\ 4D^{\circ}_{5/2}$	$4.1 \pm 0.2^f$		3.5	
37 346.31	$y\ 2F^{\circ}_{5/2}$	$3.5 \pm 0.2^f$		3.1	
37 429.76	$y\ 4F^{\circ}_{7/2}$	$4.3 \pm 0.2^f$		5.2	
37 681.75	$z\ 4S^{\circ}_{3/2}$	$4.2 \pm 0.3^b$		5.4	
37 787.59	$y\ 2F^{\circ}_{7/2}$	$4.1 \pm 0.2^f$	$4.2 \pm 0.4$	2.9	
38 041.49	$y\ 4D^{\circ}_{7/2}$	$3.3 \pm 0.2^f$		3.5	
38 063.40	$z\ 4P^{\circ}_{1/2}$			10.3	
38 133.50	$z\ 4P^{\circ}_{3/2}$	$10.6 \pm 0.3^b$		3.7	
38 482.64	$z\ 4P^{\circ}_{5/2}$			11.3	
38 644.12	$y\ 4F^{\circ}_{9/2}$	$4.9 \pm 0.2^f$		5.3	
38 934.37	$x\ 4D^{\circ}_{1/2}$	$2.3 \pm 0.1^f$		1.8	
39 192.35	$x\ 4D^{\circ}_{3/2}$	$2.3 \pm 0.1^f$		1.9	
39 640.08	$x\ 4D^{\circ}_{5/2}$	$2.3 \pm 0.1^f$		1.9	

**Table 2 – continued**

E (cm <sup>-1</sup> ) <sup>a</sup>	Designation <sup>a</sup>	$\tau$ (experiment)		$\lambda$ (theory)
		Previous work	This work	
40 238.55	$x\ 4D^{\circ}_{7/2}$	$2.4 \pm 0.1^f$		1.9
40 727.26	$y\ 2P^{\circ}_{1/2}$			5.0
40 852.74	$y\ 2G^{\circ}_{7/2}$		$3.1 \pm 0.2$	2.6
40 878.25	$y\ 2G^{\circ}_{9/2}$			3.1
41 337.36	$y\ 2P^{\circ}_{3/2}$			5.3
41 467.72	$x\ 2D^{\circ}_{3/2}$		$5.3 \pm 0.4$	4.8
41 676.82	$x\ 2D^{\circ}_{5/2}$		$5.3 \pm 0.4$	4.8
41 738.21	$z\ 2H^{\circ}_{9/2}$			3.6
42 409.93	$z\ 2H^{\circ}_{11/2}$			4.4
42 504.11	$x\ 2F^{\circ}_{7/2}$		$5.2 \pm 0.4$	4.7
42 789.24	$y\ 4P^{\circ}_{1/2}$			2.3
42 860.72	$x\ 2F^{\circ}_{5/2}$		$5.3 \pm 0.4$	4.8
42 893.54	$y\ 4P^{\circ}_{3/2}$		$2.5 \pm 0.2$	2.3
43 202.45	$y\ 4P^{\circ}_{5/2}$		$2.6 \pm 0.2$	2.2
45 054.87	$w\ 2D^{\circ}_{3/2}$			2.1
45 186.05	$w\ 2D^{\circ}_{5/2}$			2.2
45 568.21	$x\ 2P^{\circ}_{3/2}$		$7.7 \pm 0.6$	11.3
45 944.00	$x\ 2P^{\circ}_{1/2}$			11.4
47 881.88	$w\ 2F^{\circ}_{5/2}$			2.6
48 344.91	$w\ 2F^{\circ}_{7/2}$			2.5
52 585.80	$w\ 2P^{\circ}_{1/2}$			3.1
52 876.80	$w\ 2P^{\circ}_{3/2}$			3.0
55 835.53	$v\ 2D^{\circ}_{3/2}$	$0.77 \pm 0.08^e$		0.76
56 569.44	$v\ 2D^{\circ}_{5/2}$			0.76
57 062.00	$v\ 2F^{\circ}_{5/2}$	$0.88 \pm 0.08^e$		0.80
57 741.16	$v\ 2F^{\circ}_{7/2}$	$0.94 \pm 0.09^e$		0.83
60 814.50	$v\ 2P^{\circ}_{1/2}$			0.96
61 861.90	$v\ 2P^{\circ}_{3/2}$			0.93

<sup>a</sup>Moore (1958); <sup>b</sup>Biémont et al. (1981); <sup>c</sup>Hannaford & Lowe (1981); <sup>d</sup>Poulsen et al. (1982); <sup>e</sup>Sikström et al. (1999); <sup>f</sup>Langhans et al. (1995).

bars correspond to twice the standard deviation and are in the interval 2–10 per cent. We also give in Table 2 the theoretical HFR lifetime values obtained in the present work according to the procedure described hereafter (see Section 4).

Our results agree, within the error bars, with the measurements by Langhans et al. (1995) and by Biémont et al. (1981)

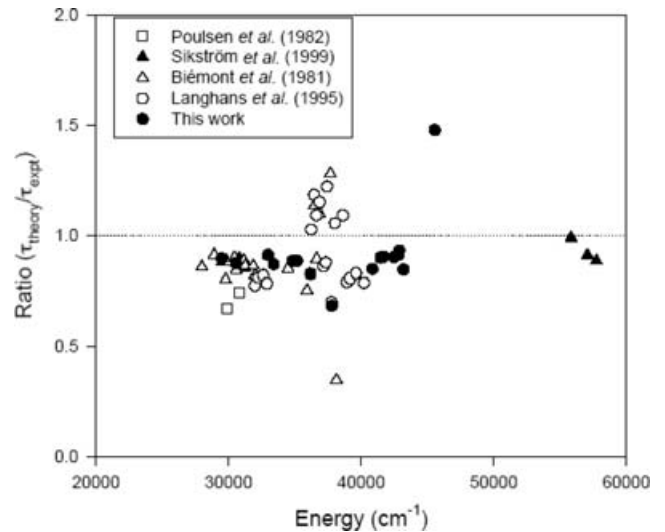


**Figure 2.** Comparison between theoretical lifetimes obtained in the present work (HFR plus CP method) and available experimental values for odd-parity levels of Zr II.

**Table 3.** Transition probabilities,  $gA$  in  $10^7 \text{ s}^{-1}$ , for lines of Zr II. Only the transitions for which  $gA$  is larger than  $5 \times 10^7 \text{ s}^{-1}$  are kept in the table.

$\lambda$ (nm) <sup>a</sup>	Lower level <sup>b</sup>		Upper level <sup>b</sup>		Intensity <sup>a</sup>	$gA^c$ (HFR)	$gA^d$ (NORM)	$gA$ (EXPT)	$gA$ (best values)	log gf (best values)
187.846	4506	5/2	57 741	7/2		108.4	95.7 <sup>e</sup>	96.5 <sup>f</sup>	96.5	-0.29
193.850	4248	3/2	55 835	3/2		106.8	105.4 <sup>e</sup>	102.4 <sup>f</sup>	102.4	-0.24
194.822	4505	5/2	55 835	3/2		41.1	40.6 <sup>e</sup>	53.4 <sup>f</sup>	53.4	-0.52
194.898	5753	5/2	57 062	5/2		103.9	94.5 <sup>e</sup>	125.9 <sup>f</sup>	125.9	-0.14
195.934	6468	7/2	57 741	7/2		84.6	74.7 <sup>e</sup>	105.2 <sup>f</sup>	105.2	-0.22
197.651	6468	7/2	57 062	5/2		14.3	13.0 <sup>e</sup>	50.3 <sup>f</sup>	50.3	-0.53
199.674	5753	5/2	55 835	3/2		139.0	137.2 <sup>e</sup>	153.3 <sup>f</sup>	153.3	-0.04
201.597	8153	9/2	57 741	7/2		75.1	66.3 <sup>e</sup>	64.8 <sup>f</sup>	64.8	-0.40
203.087	7838	7/2	57 062	5/2		56.7	51.5 <sup>e</sup>	37.3 <sup>f</sup>	37.3	-0.64
218.481	11 984	9/2	57 741	7/2		5.7	5.0 <sup>e</sup>	7.7 <sup>f</sup>	7.7	-1.26
228.863	14 060	7/2	57 741	7/2		8.2	7.2 <sup>e</sup>	7.7 <sup>f</sup>	7.7	-1.22
229.112	13 429	3/2	57 062	5/2		182.4	165.8 <sup>e</sup>	115.8 <sup>f</sup>	115.8	-0.04
229.404	14 163	5/2	57 741	7/2		398.7	352.0 <sup>e</sup>	333.2 <sup>f</sup>	333.2	0.42
229.549	14 190	9/2	57 741	7/2		165.0	145.7 <sup>e</sup>	132.2 <sup>f</sup>	132.2	0.02
232.447	14 733	5/2	57 741	7/2		44.9	39.6 <sup>e</sup>	24.7 <sup>f</sup>	24.7	-0.70
232.476	14 060	7/2	57 062	5/2		148.7	135.2 <sup>e</sup>	95.5 <sup>f</sup>	95.5	-0.11
233.035	14 163	5/2	57 062	5/2		97.7	88.8 <sup>e</sup>	95.3 <sup>f</sup>	95.3	-0.11
235.743	13 429	3/2	55 835	3/2		138.2	136.4 <sup>e</sup>	106.4 <sup>f</sup>	106.4	-0.05
239.898	14 163	5/2	55 835	3/2		13.0	12.8 <sup>e</sup>	9.8 <sup>f</sup>	9.8	-1.07
244.985	4248	3/2	45 055	3/2	150	81.8			81.8	-0.13
245.744	4506	5/2	45 186	5/2	21	115.6			115.6	0.02
248.729	8153	9/2	48 345	7/2	75	34.1			34.1	-0.50
249.648	7838	7/2	47 882	5/2	45	19.9			19.9	-0.73
253.246	763	7/2	40 239	7/2	180	26.2	20.7 <sup>g</sup>		20.7	-0.70
254.210	315	5/2	39 640	5/2	220	35.8	29.6 <sup>g</sup>		29.6	-0.54
255.074	0	3/2	39 192	3/2	220	29.3	24.2 <sup>g</sup>		24.2	-0.63
256.764	0	3/2	38 934	1/2	570	79.7	62.4 <sup>g</sup>		62.4	-0.21
256.887	1323	9/2	40 239	7/2	1600	248.9	197.0 <sup>g</sup>		197.0	0.29
257.139	763	7/2	39 640	5/2	2100	181.4	149.8 <sup>g</sup>		149.8	0.17
2572.16	315	5/2	39 192	3/2		125.4	98.1 <sup>g</sup>		98.1	-0.01
258.340	4506	5/2	43 202	5/2	75	14.9	12.6 <sup>h</sup>		12.6	-0.90
258.907	4248	3/2	42 861	5/2	130	21.2	19.2 <sup>h</sup>		19.2	-0.71
263.091	4506	5/2	42 504	7/2	150	36.7	33.1 <sup>h</sup>		33.1	-0.46
263.909	763	7/2	38 644	9/2	210	16.2	17.5 <sup>g</sup>		17.5	-0.74
265.038	763	7/2	38 483	5/2	110	8.0			8.0	-1.07
266.254	19 515	5/2	57 062	5/2		12.8	11.6 <sup>e</sup>	13.0 <sup>f</sup>	13.0	-0.86
266.780	315	5/2	37 788	7/2	180	166.7	115.1 <sup>h</sup>		115.1	0.09
267.863	1323	9/2	38 644	9/2	1800	165.7	179.2 <sup>g</sup>		179.2	0.29
268.176	763	7/2	38 041	7/2	35	16.0	16.9 <sup>g</sup>		16.9	-0.74
269.260	8058	5/2	45 186	5/2	90	14.7			14.7	-0.80
269.406	5753	5/2	42 861	5/2	180	19.7	17.9 <sup>h</sup>		17.9	-0.71
269.960	315	5/2	37 346	5/2	95	22.4	19.8 <sup>g</sup>		19.8	-0.66
270.013	763	7/2	37 788	7/2	750	83.6	57.7 <sup>h</sup>		57.7	-0.20
270.325	20 080	3/2	57 062	5/2		5.1	4.6 <sup>e</sup>	6.2 <sup>f</sup>	6.2	-1.17
271.242	315	5/2	37 171	5/2	140	40.6	34.7 <sup>g</sup>		34.7	-0.42
272.261	1323	9/2	38 041	7/2	1300	53.1	56.3 <sup>g</sup>		56.3	-0.20
272.649	763	7/2	37 430	7/2	800	28.4	34.3 <sup>g</sup>		34.3	-0.42
273.272	763	7/2	37 346	5/2	490	8.2	7.3 <sup>g</sup>		7.3	-1.09
273.486	315	5/2	36 869	5/2	1400	28.5	33.1 <sup>g</sup>		33.1	-0.43
274.051	4248	3/2	40 727	1/2	110	8.5			8.5	-1.02
274.155	1323	9/2	37 788	7/2	140	33.4	23.1 <sup>h</sup>		23.1	-0.58
274.256	0	3/2	36 452	3/2	1100	16.5	19.6 <sup>g</sup>		19.6	-0.66
274.586	763	7/2	37 171	5/2	660	42.8	36.5 <sup>g</sup>		36.5	-0.38
275.221	315	5/2	36 639	3/2	660	15.6	17.1 <sup>g</sup>		17.1	-0.71
275.251	19 515	5/2	55 835	3/2		31.7	31.3 <sup>e</sup>	22.2 <sup>f</sup>	22.2	-0.60
276.000	19 614	1/2	55 835	3/2		12.8	12.6 <sup>e</sup>	6.2 <sup>f</sup>	6.2	-1.15
276.191	0	3/2	36 197	1/2	70	22.9	19.2 <sup>h</sup>		19.2	-0.66
276.873	1323	9/2	37 430	7/2	200	29.6	35.8 <sup>g</sup>		35.8	-0.39
276.885	763	7/2	36 869	5/2		21.9	25.3 <sup>g</sup>		25.3	-0.54
277.416	6468	7/2	42 504	7/2		23.4	21.2 <sup>h</sup>		21.2	-0.61
279.690	5724	1/2	41 468	3/2	160	5.8	5.2 <sup>h</sup>		5.2	-1.21

Table 3 – continued

$\lambda$ (nm) <sup>a</sup>	Lower level <sup>b</sup>		Upper level <sup>b</sup>		Intensity <sup>a</sup>	gA <sup>c</sup> (HFR)	gA <sup>d</sup> (NORM)	gA (EXPT)	gA (best values)	log gf (best values)
281.091	6112	3/2	41 677	5/2	180	32.5	29.4 <sup>h</sup>		29.4	-0.46
281.874	7736	3/2	43 202	5/2	390	73.4	62.1 <sup>h</sup>		62.1	-0.13
282.556	7513	1/2	42 894	3/2	530	71.4	65.7 <sup>h</sup>		65.7	-0.10
283.391	7513	1/2	42 789	1/2	110	13.5			13.5	-0.79
283.440	6468	7/2	41 738	9/2	80	8.3			8.3	-1.00
283.802	6112	3/2	41 337	3/2	55	5.9			5.9	-1.15
283.934	6468	7/2	41 677	5/2	120	13.5	12.3 <sup>h</sup>		12.3	-0.83
284.352	7736	3/2	42 894	3/2	130	24.5	22.6 <sup>h</sup>		22.6	-0.56
284.458	8058	5/2	43 202	5/2	660	161.5	136.6 <sup>h</sup>		136.6	0.22
284.819	5753	5/2	40 853	7/2	210	20.1	16.9 <sup>h</sup>		16.9	-0.69
285.197	7736	3/2	42 789	1/2	350	69.1			69.1	-0.07
285.443	7838	7/2	42 861	5/2	70	6.3	5.7 <sup>h</sup>		5.7	-1.16
286.981	8058	5/2	42 894	3/2	340	68.3	62.8 <sup>h</sup>		62.8	-0.11
288.380	7838	7/2	42 504	7/2	55	9.1	8.3 <sup>h</sup>		8.3	-0.99
288.804	6112	3/2	40 727	1/2	90	5.5			5.5	-1.16
289.871	3300	7/2	37 788	7/2	90	5.5	3.8 <sup>h</sup>		3.8	-1.32
290.162	13 428	3/2	47 882	5/2	60	19.8			19.8	-0.60
290.523	6468	7/2	40 878	9/2	160	20.3			20.3	-0.59
290.738	6468	7/2	40 853	7/2	70	7.7	6.5 <sup>h</sup>		6.5	-1.08
291.025	8153	9/2	42 504	7/2	90	9.2	8.3 <sup>h</sup>		8.3	-0.98
291.599	3758	9/2	38 041	7/2	300	17.7	18.8 <sup>g</sup>		18.8	-0.62
291.664	2895	5/2	37 171	5/2	110	6.0	5.2 <sup>g</sup>		5.2	-1.18
291.824	8153	9/2	42 410	11/2	270	61.4			61.4	-0.11
292.464	14 163	5/2	48 345	7/2	45	17.1			17.1	-0.66
292.699	14 190	9/2	48 345	7/2	320	217.3			217.3	0.45
293.631	3300	7/2	37 346	5/2	160	7.8	6.9 <sup>g</sup>		6.9	-1.05
294.546	7736	3/2	41 677	5/2	90	5.8	5.3 <sup>h</sup>		5.3	-1.16
294.894	7838	7/2	41 738	9/2	320	42.2			42.2	-0.26
295.578	14 060	7/2	47 882	5/2	320	155.8			155.8	0.31
296.896	3758	9/2	37 430	7/2	320	38.7	46.8 <sup>g</sup>		46.8	-0.21
297.661	8153	9/2	41 738	9/2	130	30.6			30.6	-0.39
297.805	3300	7/2	36 869	5/2	320	30.1	34.9 <sup>g</sup>		34.9	-0.33
297.918	2895	5/2	36 452	3/2	230	26.1	30.6 <sup>g</sup>		30.6	-0.39
298.102	4506	5/2	38 041	7/2	160	30.5	32.3 <sup>g</sup>		32.3	-0.37
302.047	4248	3/2	37 346	5/2	350	24.2	21.4 <sup>g</sup>		21.4	-0.53
302.804	7838	7/2	40 853	7/2	500	70.8	59.4 <sup>h</sup>		59.4	-0.09
303.092	0	3/2	32 984	3/2	180	5.5	5.0 <sup>h</sup>		5.0	-1.16
303.639	4506	5/2	37 430	7/2	350	23.9	28.9 <sup>g</sup>		28.9	-0.40
305.484	8153	9/2	40 878	9/2	690	85.3			85.3	0.08
305.722	8153	9/2	40 853	7/2	70	8.5	7.1 <sup>h</sup>		7.1	-1.00
306.463	4248	3/2	36 869	5/2	100	7.9	9.2 <sup>g</sup>		9.2	-0.89
309.507	315	5/2	32 615	5/2	250	13.2	10.7 <sup>g</sup>		10.7	-0.81
309.923	0	3/2	32 257	3/2	280	9.9	8.0 <sup>e</sup>		8.0	-0.94
310.658	8058	5/2	40 239	7/2	690	129.5	102.5 <sup>g</sup>		102.5	0.17
311.088	763	7/2	32 899	7/2	210	14.2	11.1 <sup>g</sup>		11.1	-0.79
312.519	4248	3/2	36 237	1/2	70	40.4	41.6 <sup>g</sup>		41.6	-0.22
312.592	0	3/2	31 981	1/2	320	17.2	13.3 <sup>g</sup>		13.3	-0.71
312.976	315	5/2	32 257	3/2	500	22.2	18.1 <sup>e</sup>		18.1	-0.58
313.348	7736	3/2	39 640	5/2	350	67.9	56.1 <sup>g</sup>		56.1	-0.08
313.868	763	7/2	32 615	5/2	690	31.0	25.2 <sup>g</sup>		25.2	-0.43
315.567	7513	1/2	39 192	3/2	290	28.1	23.2 <sup>g</sup>		23.2	-0.46
315.700	4248	3/2	35 915	3/2	150	9.9	7.4 <sup>i</sup>		7.4	-0.96
316.431	5753	5/2	37 346	5/2	540	40.8	36.2 <sup>g</sup>		36.2	-0.26
316.545	8058	5/2	39 640	5/2	150	16.9	14.0 <sup>g</sup>		14.0	-0.68
316.597	1323	9/2	32 899	7/2	880	53.3	41.6 <sup>g</sup>		41.6	-0.20
316.626	6468	7/2	38 041	7/2	150	45.6	48.3 <sup>g</sup>		48.3	-0.14
317.809	7736	3/2	39 192	3/2	190	22.8	18.8 <sup>g</sup>		18.8	-0.54
318.158	7513	1/2	38 934	1/2	190	22.5	17.6 <sup>g</sup>		17.6	-0.57
318.286	4506	5/2	35 915	3/2	880	87.6	65.1 <sup>i</sup>		65.1	-0.00
321.285	5753	5/2	36 869	5/2	75	14.7	17.0 <sup>g</sup>		17.0	-0.58
321.419	763	7/2	31 866	9/2	760	31.7	26.9 <sup>i</sup>		26.9	-0.38
322.881	6468	7/2	37 430	7/2	200	26.1	31.5 <sup>g</sup>		31.5	-0.31
323.169	315	5/2	31 249	7/2	630	29.6	25.2 <sup>e</sup>		25.2	-0.40

Table 3 – continued

$\lambda$ (nm) <sup>a</sup>	Lower level <sup>b</sup>		Upper level <sup>b</sup>		Intensity <sup>a</sup>	gA <sup>c</sup> (HFR)	gA <sup>d</sup> (NORM)	gA (EXPT)	gA (best values)	log gf (best values)
323.658	14 299	3/2	45 186	5/2	110	7.9			7.9	−0.91
324.105	315	5/2	31 160	5/2	760	14.6	12.9 <sup>i</sup>		12.9	−0.69
325.046	14 299	3/2	45 055	3/2		58.2			58.2	−0.04
326.481	7513	1/2	38 134	3/2	40	17.8	6.2 <sup>i</sup>		6.2	−1.00
327.113	4248	3/2	34 810	1/2	150	8.1	7.1 <sup>h</sup>		7.1	−0.94
327.222	0	3/2	30 551	5/2	540	20.2			20.2	−0.49
327.305	1323	9/2	31 866	9/2	1000	138.4	117.3 <sup>i</sup>		117.3	0.28
327.926	763	7/2	31 249	7/2	1300	82.5	70.2 <sup>e</sup>		70.2	0.05
328.283	14 733	5/2	45 186	5/2		92.0			92.0	0.17
328.471	0	3/2	30 435	3/2	880	24.4	22.1 <sup>i</sup>		22.1	−0.45
328.588	8058	5/2	38 483	5/2	140	20.9			20.9	−0.47
329.640	7736	3/2	38 063	1/2	75	8.2			8.2	−0.87
330.267	9969	5/2	40 239	7/2	75	10.1	8.0 <sup>g</sup>		8.0	−0.88
330.515	315	5/2	30 562	7/2	540	10.6	9.3 <sup>h</sup>		9.3	−0.82
330.628	315	5/2	30 551	5/2	880	40.9			40.9	−0.17
330.989	7838	7/2	38 041	7/2	40	7.3	7.8 <sup>g</sup>		7.8	−0.89
331.450	5753	5/2	35 915	3/2	210	14.0	10.4 <sup>i</sup>		10.4	−0.77
331.851	6112	3/2	36 237	1/2	75	17.5	18.0 <sup>g</sup>		18.0	−0.53
332.680	12 360	11/2	42 410	11/2	380	55.5			55.5	−0.04
333.425	8058	5/2	38 041	7/2	380	18.7	19.8 <sup>g</sup>		19.8	−0.48
333.462	4506	5/2	34 485	7/2	210	13.2	11.3 <sup>i</sup>		11.3	−0.72
334.056	1323	9/2	31 249	7/2	760	20.9	17.8 <sup>e</sup>		17.8	−0.53
334.479	8153	9/2	38 041	7/2	380	56.6	60.1 <sup>g</sup>		60.1	0.00
335.439	6112	3/2	35 915	3/2	180	11.6	8.6 <sup>i</sup>		8.6	−0.84
335.609	763	7/2	30 551	5/2	760	24.1			24.1	−0.39
335.726	0	3/2	29 778	3/2	540	19.8	15.7 <sup>i</sup>		15.7	−0.58
335.996	11 984	9/2	41 738	9/2	180	30.9			30.9	−0.28
336.268	8058	5/2	37 788	7/2	95	7.6	5.3 <sup>h</sup>		5.3	−1.05
337.473	8058	5/2	37 682	3/2	380	38.1	49.0 <sup>i</sup>		49.0	−0.08
337.627	7736	3/2	37 346	5/2	110	5.2	4.6 <sup>g</sup>		20.9	−1.10
338.787	7838	7/2	37 346	5/2	570	55.4	49.0 <sup>g</sup>		8.2	−0.07
338.830	0	3/2	29 505	5/2	760	17.4	15.5 <sup>h</sup>		15.5	−0.57
339.198	1323	9/2	30 796	11/2	5700	237.6	211.2 <sup>e</sup>		211.2	0.56
339.312	315	5/2	29 778	3/2	570	14.2	11.3 <sup>i</sup>		11.3	−0.71
339.633	7736	3/2	37 171	5/2	160	6.5	5.5 <sup>g</sup>		5.5	−1.02
339.666	13 429	3/2	42 861	5/2	40	26.0	23.5 <sup>h</sup>		23.5	−0.39
339.935	2572	3/2	31 981	1/2	380	13.4	10.4 <sup>g</sup>		10.4	−0.74
340.287	12 360	11/2	41 738	9/2	150	57.3			57.3	−0.00
340.368	8058	5/2	37 430	7/2	190	34.8	42.1 <sup>g</sup>		42.1	−0.14
340.483	2895	5/2	32 257	3/2	570	23.3	18.9 <sup>e</sup>		18.9	−0.48
341.025	3300	7/2	32 615	5/2	760	34.4	28.0 <sup>g</sup>		28.0	−0.31
343.053	3758	9/2	32 899	7/2	1000	51.5	40.2 <sup>g</sup>		40.2	−0.15
343.157	7736	3/2	36 869	5/2	110	21.0	24.4 <sup>g</sup>		24.4	−0.37
343.714	5724	1/2	34 810	1/2	380	22.1	19.4 <sup>h</sup>		19.4	−0.46
343.823	763	7/2	29 840	9/2	4700	160.1	143.2 <sup>i</sup>		143.2	0.40
344.357	7838	7/2	36 869	5/2	120	17.0	19.7 <sup>g</sup>		19.7	−0.46
345.756	4506	5/2	33 419	5/2	410	21.8	18.8 <sup>h</sup>		18.8	−0.47
346.302	11 984	9/2	40 853	7/2	820	134.3	112.6 <sup>h</sup>		112.6	0.31
346.994	8058	5/2	36 869	5/2	40	10.5	12.2 <sup>g</sup>		12.2	−0.66
347.850	9743	3/2	38 483	5/2	65	7.8			7.8	−0.85
347.902	4248	3/2	32 984	3/2	180	13.7	12.4 <sup>h</sup>		11.2 <sup>j</sup>	−0.69
347.939	5753	5/2	34 485	7/2	1200	92.2	78.8 <sup>i</sup>	81.4 <sup>j</sup>	81.4	0.17
348.115	6468	7/2	35 186	9/2	1300	122.0	106.4 <sup>h</sup>		106.4	0.29
348.354	6112	3/2	34 810	1/2	760	23.3	20.5 <sup>h</sup>		20.5	−0.43
348.532	7513	1/2	36 197	1/2	130	12.5	10.5 <sup>h</sup>		10.5	−0.72
349.621	315	5/2	28 909	7/2	4100	106.2	97.4 <sup>i</sup>		97.4	0.25
349.958	3300	7/2	31 866	9/2	190	5.4	4.6 <sup>i</sup>	8.4 <sup>j</sup>	8.4	−0.81
350.548	12 360	11/2	40 878	9/2	350	104.7			104.7	0.29
350.567	1323	9/2	29 840	9/2	820	26.8	24.0 <sup>i</sup>	23.6 <sup>j</sup>	23.6	−0.36
350.605	9969	5/2	38 483	5/2	80	11.3			11.3	−0.68
351.046	4506	5/2	32 984	3/2	200	5.4	4.9 <sup>h</sup>		4.9	−1.04
352.581	2895	5/2	31 249	7/2	440	7.9	6.7 <sup>e</sup>		6.7	−0.90
353.085	14 190	9/2	42 504	7/2	70	24.4	22.1 <sup>h</sup>		22.1	−0.38

**Table 3** – *continued*

$\lambda$ (nm) <sup>a</sup>	Lower level <sup>b</sup>		Upper level <sup>b</sup>		Intensity <sup>a</sup>	gA <sup>c</sup> (HFR)	gA <sup>d</sup> (NORM)	gA (EXPT)	gA (best values)	log gf (best values)
354.262	14 190	9/2	42 410	11/2	630	145.5			145.5	0.44
354.951	9969	5/2	38 134	3/2	130	32.9	11.5 <sup>i</sup>	21.1 <sup>j</sup>	21.1	-0.40
355.195	763	7/2	28 909	7/2	1800	27.3	25.0 <sup>i</sup>	25.9 <sup>j</sup>	25.9	-0.31
355.407	9553	1/2	37 682	3/2	130	14.3	18.4 <sup>i</sup>		18.4	-0.46
355.660	3758	9/2	31 866	9/2	2100	78.0	66.1 <sup>i</sup>		66.1	0.10
357.247	0	3/2	27 984	5/2	2100	66.5	57.2 <sup>i</sup>		57.2	0.04
357.308	2572	3/2	30 551	5/2	210	6.4			6.4	-0.91
357.685	3300	7/2	31 249	7/2	1300	54.7	46.6 <sup>e</sup>		46.6	-0.05
357.823	9743	3/2	37 682	3/2	150	11.7	15.1 <sup>i</sup>		15.1	-0.54
358.798	2572	3/2	30 435	3/2	440	5.7	5.1 <sup>i</sup>		5.1	-1.01
361.189	14 060	7/2	41 738	9/2	690	94.6			94.6	0.27
361.310	315	5/2	27 984	5/2	1100	15.8	13.6 <sup>i</sup>		13.6	-0.57
361.477	2895	5/2	30 551	5/2	1100	36.6			36.6	-0.14
363.349	14 163	5/2	41 677	5/2	140	14.1	12.8 <sup>h</sup>		12.8	-0.60
366.214	13 429	3/2	40 727	1/2	95	17.7			17.7	-0.45
367.127	5753	5/2	32 984	3/2	390	14.9	13.5 <sup>h</sup>	12.4 <sup>j</sup>	12.4	-0.60
367.472	2572	3/2	29 778	3/2	800	22.9	18.1 <sup>i</sup>		18.1	-0.44
369.746	3758	9/2	30 796	11/2	390	11.0	9.8 <sup>e</sup>		9.8	-0.70
369.817	8153	9/2	35 186	9/2	960	87.1	75.9 <sup>h</sup>		75.9	0.19
370.926	6468	7/2	33 419	5/2	720	33.5	29.0 <sup>h</sup>		29.0	-0.22
371.478	4248	3/2	31 160	5/2	190	5.8	5.1 <sup>i</sup>	5.7 <sup>j</sup>	5.7	-0.93
373.126	14 060	7/2	40 853	7/2	270	49.2	41.3 <sup>h</sup>		41.3	-0.06
374.598	14 190	9/2	40 878	9/2	560	62.1			62.1	0.12
375.160	7838	7/2	34 485	7/2	880	60.4	51.6 <sup>i</sup>		51.6	0.04
376.682	3300	7/2	29 840	9/2	340	9.5	8.5 <sup>i</sup>		8.5	-0.74
379.648	8153	9/2	34 485	7/2	130	8.5	7.3 <sup>i</sup>	6.8 <sup>j</sup>	6.8	-0.84
381.758	4248	3/2	30 435	3/2	210	7.3	6.6 <sup>i</sup>		6.6	-0.84
383.676	4506	5/2	30 562	7/2	1300	42.9	37.5 <sup>h</sup>	39.4 <sup>j</sup>	39.4	-0.06
384.302	2895	5/2	28 909	7/2	550	7.0	6.4 <sup>i</sup>		6.4	-0.85
391.434	19 515	5/2	45 055	3/2	40	13.3			13.3	-0.51
391.594	4248	3/2	29 778	3/2	310	5.2	4.1 <sup>i</sup>		4.1	-1.03
393.479	5753	5/2	31 160	5/2	200	6.8	6.0 <sup>i</sup>		6.0	-0.86
395.822	4248	3/2	29 505	5/2	940	26.0	23.1 <sup>h</sup>		23.1	-0.27
399.113	6112	3/2	31 160	5/2	770	28.3	24.9 <sup>i</sup>		24.9	-0.23
399.897	4506	5/2	29 505	5/2	770	16.8	14.9 <sup>h</sup>		14.9	-0.45
402.968	5753	5/2	30 562	7/2	400	8.6	7.5 <sup>h</sup>		7.5	-0.74
404.561	5724	1/2	30 435	3/2	400	10.3	9.3 <sup>i</sup>		9.3	-0.64
404.867	6468	7/2	31 160	5/2	610	15.5	13.6 <sup>i</sup>		13.6	-0.48
405.033	5753	5/2	30 435	3/2	200	7.4	6.7 <sup>i</sup>	4.1 <sup>j</sup>	4.1	-1.00
414.920	6468	7/2	30 562	7/2	1200	45.1	39.4 <sup>h</sup>	36.1 <sup>j</sup>	36.1	-0.03
415.624	5724	1/2	29 778	3/2	290	5.4	4.2 <sup>i</sup>		4.2	-0.96
416.121	5753	5/2	29 778	3/2	400	9.3	7.4 <sup>i</sup>	7.3 <sup>j</sup>	7.3	-0.72
417.981	13 429	3/2	37 346	5/2	75	5.5	4.9 <sup>g</sup>		4.9	-0.89
418.669	14 163	5/2	38 041	7/2	100	7.0	7.4 <sup>g</sup>		7.4	-0.71
420.898	5753	5/2	29 505	5/2	610	14.5	12.8 <sup>h</sup>	13.0 <sup>j</sup>	13.0	-0.46
433.326	19 433	7/2	42 504	7/2	40	17.0	15.4 <sup>h</sup>		15.4	-0.36
435.974	9969	5/2	32 899	7/2	290	17.4	13.5 <sup>g</sup>		13.5	-0.41
437.095	9743	3/2	32 615	5/2	130	8.7	7.1 <sup>g</sup>		7.1	-0.69
437.978	12 360	11/2	35 186	9/2	240	22.4	19.6 <sup>h</sup>		19.6	-0.25
444.300	11 984	9/2	34 485	7/2	140	16.8	14.3 <sup>i</sup>	15.8 <sup>j</sup>	15.8	-0.33
449.442	19 433	7/2	41 677	5/2	55	21.4	19.4 <sup>h</sup>		19.4	-0.23
462.907	20 080	3/2	41 677	5/2	40	13.5	12.3 <sup>h</sup>		12.3	-0.40
468.519	19 515	5/2	40 853	7/2	23	8.9	7.5 <sup>h</sup>		7.5	-0.61
535.009	14 733	5/2	33 419	5/2	30	11.0	9.5 <sup>h</sup>		9.5	-0.39
535.035	14 299	3/2	32 984	3/2	30	6.2	5.6 <sup>h</sup>		5.6	-0.62

<sup>a</sup>from Meggers et al. (1975) and Sikström et al. (1999); <sup>b</sup>from Moore (1958); <sup>c</sup>this work (HFR calculations); <sup>d</sup>this work (HFR calculations normalized with available experimental lifetimes); <sup>e</sup>gA values normalized using the experimental lifetimes obtained by Sikström et al. (1999); <sup>f</sup>Deduced from f values obtained from experimental lifetimes and FTS BF measurements by Sikström et al. (1999); <sup>g</sup>gA values normalized using the experimental lifetimes obtained by Langhans et al. (1995); <sup>h</sup>gA values normalized using the experimental lifetimes obtained in the present work; <sup>i</sup>gA values normalized using the experimental lifetimes obtained by Biémont et al. (1981); <sup>j</sup>Deduced from f values obtained from experimental lifetimes and FTS BF measurements by Biémont et al. (1981).

(for four levels) which were also obtained using selective laser excitation.

#### 4 THEORETICAL MODEL

The relativistic Hartree–Fock (HFR) method, as described by Cowan (1981), was used to compute radiative lifetimes and BFs for the transitions depopulating the odd-parity levels of Zr II. In the physical model adopted, we supposed that the Zr<sup>+</sup> ion could be represented by three valence electrons surrounding a Kr-like ionic core with 36 electrons occupying closed subshells of the type  $1s^2 2s^2 2p^6 3s^2 3p^6 3d^{10} 4s^2 4p^6$ . The intravalence correlation was then considered by the explicit introduction, in the HFR calculations, of the following interacting configurations:  $4d5s^2 + 4d5p^2 + 4d5d^2 + 4d4f^2 + 4d5f^2 + 4d5s6s + 4d5s5d + 4d5s6d + 4d5p4f + 4d5p5f + 4d^2 5s + 4d^2 6s + 4d^2 5d + 4d^2 6d + 4d^3 + 5s^2 6s + 5s^2 5d + 5s^2 6d$  (even parity) and  $4d5s5p + 4d5s6p + 4d5s4f + 4d5s5f + 4d5p5d + 4d5d4f + 4d5d5f + 4d^2 5p + 4d^2 6p + 4d^2 4f + 4d^2 5f + 5s^2 5p + 5s^2 6p + 5s^2 4f + 5s^2 5f$  (odd parity).

Core–valence correlation was considered by including in the HFR method a core-polarization (CP) potential and a correction to the dipole operator as it has been described in many previous papers (see e.g. Quinet et al. 1999; Biémont et al. 2000). These corrections were used with a value of the dipole polarizability equal to  $2.98a_0^3$ , as computed by Johnson, Kolb & Huang (1983), for the Kr-like Zr<sup>4+</sup> ion. A cut-off radius equal to  $1.35a_0$ , which corresponds to the HFR expectation value of  $\langle r \rangle$  for the outermost core orbital, i.e. 4p, was retained for the calculations.

This HFR plus CP method was then combined with a least-squares optimization of the radial parameters in order to minimize the discrepancies between calculated energy levels and experimental values when available. More precisely, the 35 even-parity experimental levels reported by Moore (1958) as belonging to  $4d5s^2$ ,  $4d^2 5s$  and  $4d^3$  were used to adjust the numerical values of the average energies ( $E_{av}$ ) of the electrostatic ( $F^k$ ,  $G^k$ ) and the spin–orbit integrals ( $\zeta_{nl}$ ) together with the effective interaction parameters ( $\alpha$ ,  $\beta$ ) corresponding to these three configurations. Similarly, the 68 odd-parity levels, taken from the same compilation, were used to optimize all the radial parameters, including the interaction configuration integrals ( $R^k$ ), corresponding to the  $4d5s5p$  and  $4d^2 5p$  configurations. The standard deviations of the fitting procedures were found to be equal to  $46 \text{ cm}^{-1}$  (35 levels, 15 adjustable parameters) for the even parity and  $177 \text{ cm}^{-1}$  (68 levels, 19 variable parameters) for the odd parity.

#### 5 DISCUSSION OF THE RESULTS

Radiative lifetimes, as obtained with the HFR plus CP method, are reported in the last column of Table 2 where they are compared with available experimental values. Inspection of the data in Table 2 reveals that, with the exception of the  $z^4 P^{\circ}_{3/2}$  level at  $38\,133.50 \text{ cm}^{-1}$ , we observe a good agreement between theory and experiment. However, the HFR lifetimes seem to be generally smaller than the measurements as illustrated in Fig. 2. This could be explained by the fact that the core-polarization effects are underestimated in the physical model used in the present work. The use of the dipole polarizability published by Fraga, Karwowski & Saxena (1976), i.e.  $\alpha_d = 3.24 \text{ au}$ , instead of the one reported by Johnson et al. (1983), did not improve upon the situation. Indeed, it was found that, when using the former value, the calculated lifetimes did increase by only about 1 per cent. Large discrepancies between theory and experiment are observed for only two levels, at  $38\,133.50 \text{ cm}^{-1}$  ( $z^4 P^{\circ}_{3/2}$ ) and  $45\,568.21 \text{ cm}^{-1}$

( $x^2 P^{\circ}_{3/2}$ ), respectively. As the two experimental values were obtained with a LIF technique, the problem is probably occurring on the theoretical side. No precise explanation, however, could be found.

Calculated HFR plus CP transition probabilities and ‘normalized’ values (obtained by combining HFR plus CP BFs and the most accurate available experimental lifetimes) are presented in Table 3. These normalized gA values (we limited the table to gA values larger than  $5 \times 10^7 \text{ s}^{-1}$  because calculated BFs are expected to be more accurate for intense than for weak transitions) are compared with the experimental results obtained by Biémont et al. (1981) and Sikström et al. (1999) who combined radiative lifetimes measured by laser spectroscopy and BFs determined from intensity measurements on laboratory spectra.

The normalized gA values agree quite well [ $<10$  per cent] with the experimental results of Biémont et al. (1981) and this agreement gives some weight to the calculated BFs. The only exception is the transition at  $354.951 \text{ nm}$  where a discrepancy of a factor of 2 is observed. This agreement is confirmed when plotting the HFR gf values versus the results of Grevesse et al. (1981) (see Fig. 3). This figure shows that the two sets of results agree quite well if we exclude the two weak transitions at  $535.009$  and  $535.035 \text{ nm}$  but, for these two transitions, the BFs in the work of Grevesse et al. (1981) were taken directly from the work of Corliss & Bozman (1962) and were not remeasured by these authors.

The comparison of the normalized gA values with the results of Sikström et al. (1999) leads to less obvious conclusions. For 14 transitions, the agreement is within 35 per cent but larger discrepancies are observed for the remaining transitions. It should be pointed out, however, that the uncertainties of the results of Sikström et al. (1999) are estimated by the authors to be within 25 and 40 per cent and depend on the difficulties related to both the intensity measurements and the intensity calibration.

We give, in the last column of the Table 3, the ‘best’ values that we suggest to use. They correspond, in order of expected decreasing accuracy, to experimental LIF lifetimes combined with laboratory BFs, to experimental LIF lifetimes combined with HFR BFs and, finally, to HFR plus CP transition probabilities. For most of the transitions, the accuracy of the transition probabilities is expected

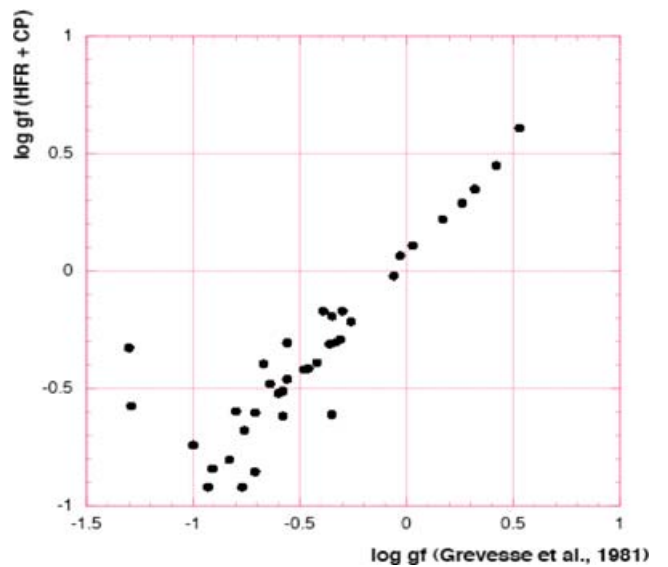


**Figure 3.** Comparison between Zr II theoretical gf values obtained in the present work (HFR plus CP method) and available experimental results (Grevesse et al. 1981).



to be within 20 per cent. It could be larger for erratic transitions in relation to possible cancellation effects appearing in the calculation of the line strengths.

In conclusion, we present in this paper an extensive set of transition probabilities in Zr II for 243 transitions of astrophysical interest appearing in the UV and visible regions. Their accuracy is assessed through comparisons with available experimental measurements. The present data improves the gap in the atomic data base for the Zr II ion, but additional efforts are required in this field.

## ACKNOWLEDGMENTS

This work was financially supported by the Swedish Research Council and by the EU-TMR access to Large-Scale Facility Programme (contract RII3-CT-2003-506350). E. Biémont and P. Quinet are Research Director and Research Associate of the Belgian FNRS. Financial support from this organization is acknowledged. The experimental part of this work was supported by the Academic Exchange Programme between the Consejo Superior de Investigaciones Científicas-Universidad Complutense de Madrid and the Bulgarian Academy of Sciences. National Science Fund of Bulgaria is acknowledged for financial support (grant 1516/05).

## REFERENCES

- Adelman S., 1973, *ApJS*, 26, 1  
 Allen M. S., 1976, *PASP*, 88, 338  
 Bell R. A., Upson W. L. II, 1971, *Astrophys. Lett.*, 9, 109  
 Biémont É., Grevesse N., Hannaford P., Lowe R. M., 1981, *ApJ*, 248, 867  
 Biémont É., Froese Fischer C., Godefroid M. R., Palmeri P., Quinet P., 2000, *Phys. Rev. A*, 62, 032512  
 Biémont É., Quinet P., Svanberg S., Xu H. L., 2004, *J. Phys. B: At. Mol. Phys.*, 37, 1381  
 Bogdanovich P., Tautvaisiene G., Rudzikas Z., Momkauskaitė A., 1995, *MNRAS*, 280, 95  
 Boyarchuk M. E., Boyarchuk A. A., 1960, *Izv. Krym. Astrofis. Obs. (Russ.)*, 22, 234  
 Corliss C. H., Bozman W. R., 1962, *Experimental Transition Probabilities for Spectral Lines of Seventy Elements*, Nat. Bur. Stand. (US), Monograph 53, Washington, DC  
 Corliss C. H., Tech J. L., 1976, *J. Res. Nat. Bur. Stand.*, A80, 787  
 Cowan R. D., 1981, *The Theory of Atomic Structure and Spectra*. University of California Press, Berkeley, USA  
 Cowley C. R., 1976, *ApJS*, 32, 631  
 Cowley C. R., 1983, *MNRAS*, 202, 417  
 Cowley C. R., Aikman G. C. L., 1975, *ApJ*, 196, 521  
 Cowley C. R., Corliss C. H., 1983, *MNRAS*, 203, 651  
 Fraga S., Karwowski J., Saxena K. M. S., 1976, *Handbook of Atomic Data*. Elsevier, Amsterdam  
 Grevesse N., Biémont E., Hannaford P., Lowe R. M., 1981, in *Upper Main Sequence CP Stars*, 23rd Liège Astrophys. Coll., University of Liège  
 Hannaford P., Lowe R. M., 1981, *J. Phys. B: At. Mol. Phys.*, B14, L5  
 Johnson W. R., Kolb D., Huang K. N., 1983, *At. Data Nucl. Data Tables*, 28, 333  
 Kodaira K., Takada M., 1978, *Ann. Tokyo Obs. Second Ser.*, 17, 79  
 Langhans G., Schade W., Helbig V., 1995, *Z. Phys.*, D34, 151  
 Luck R. E., Bond H. E., 1981, *ApJ*, 244, 919  
 Malloy P. J., Czyzak S. J., 1978, *Ap&SS*, 58, 365  
 Meggers W. F., Corliss C. H., Scribner B. F., 1975, *Tables of Spectral Line Intensities*, NBS Monograph 145, Part 1, Washington, DC  
 Meylan T., Furenlid I., Wiggs M. S., Kurucz R. L., 1993, *ApJS*, 85, 163  
 Moore C. E., 1958, *Atomic Energy Levels*, NBS Circular 467, Vol. 3, Washington, DC  
 Pirronello V., Strazzulla G., 1980, *Ap&SS*, 72, 55  
 Poulsen O., Andersen T., Bentzen S. M., Koleva I., 1982, *Nucl. Instrum. Methods*, 202, 139  
 Quinet P., Palmeri P., Biémont E., McCurdy M. M., Rieger G., Pinnington E. H., Wickliffe M. E., Lawler J. E., 1999, *MNRAS*, 307, 934  
 Sikström C. M., Lundberg H., Wahlgren G. M., Li Z. S., Lyngå C., Johansson S., Leckrone D. S., 1999, *A&A*, 343, 297  
 Sadakane K., 1976, *PASP Japan*, 28, 469  
 Thevenin F., 1989, *A&AS*, 77, 137  
 Thevenin F., 1990, *A&AS*, 82, 179  
 Xu H. L. et al., 2004, *Phys. Rev. A*, 70, 042508

This paper has been typeset from a MS Word file prepared by the author.